The 9th European Congress on Computational Methods in Applied Sciences and Engineering
ECCOMAS Congress 2024
3–7 June 2024, Lisboa, Portugal

THERMAL EFFECTS ON NONLINEAR OSCILLATIONS OF HARD-MAGNETIC SOFT ACTUATORS

SHIVENDRA NANDAN[1], DIVYANSH SHARMA[2] AND ATUL KUMAR SHARMA[1]

[1,2,3] Soft Active Materials and Structures Laboratory
Department of Mechanical Engineering
Indian Institute of Technology Jodhpur 342037, India
e-mail: atulksharma@iitj.ac.in (Corresponding Author),
https://sites.google.com/iitj.ac.in/atul-kumar-sharma

Key words: Hard-magnetic soft materials, Soft actuator, Viscoelasticity, Nonlinear oscillations,Poincaré maps

Summary. *In recent years, there has been a growing interest in hard-magnetic soft materials (HMSMs) due to their capacity to retain high residual magnetization and undergo significant deformation when subjected to external magnetic loading. The performance of these materials in dynamic actuation modes is substantially affected by temperature. This article introduces a theoretical framework for modeling the dynamic behavior of hard-magnetic soft materials. The neo-Hookean material model is employed to account for the thermal properties of the HSM materials. The governing equation for dynamic motion is derived using Euler-Lagrange's principle for nonconservative systems, allowing the characterization of nonlinear oscillations under both constant and periodic magnetic fluxes. Dynamic stability, resonance properties, dynamic response, and periodicity are characterized using frequency response spectra, time history graphs, phase-plane diagrams, and Poincaré maps. The investigation seeks to comprehend the transition from periodic to quasi-periodic oscillation behavior of actuators. These findings represent an initial step towards designing and developing remotely controlled actuators for various futuristic applications.*

1 Introduction

Soft magnetoactive polymers (SMAPs), a class of smart soft active materials, undergo large mechanical deformation when subjected to an external magnetic field and are classified based on the composition and arrangement of their magnetic components, such as magnetic particle-based, magnetic fiber-based, ferrogel-based, and magnetic liquid crystal elastomers. In recent years, Hard-magnetic soft materials have gained significant attention due to their exceptional properties, including their response to external stimuli, quick actuation, flexibility, and stretchability, and have a wide range of potential applications, such as in soft robotics, actuators, microfluidics, and biomedical devices. These materials typically embed neodymium-iron-boron (NdFeB) microparticles into the soft matrix. These magnetic particles can retain their magnetism even after removal of the external magnetic field due to their high remanence, which allows them to retain a strong magnetic moment density along desired directions (i.e., vertical,

horizontal, and inclined directions). The HMS actuators generally experience very large and nonlinear deformation, which significantly affects the inherent properties of the material.

The primary characteristic of HMSMs is that when a relatively small magnetic induction is applied externally, it results in instantaneous and significant deformations of the magnetorheological elastomer [14, 23]. To present the recent developments in continuum theories of HMS materials, Kalina et al. [9] and Zhao et al. [28] investigated the structural properties of the soft magnetorheological elastomers to model the magnetic hystereses. The HMS materials exhibit time-dependent deformation relying on the viscoelasticity of the polymer matrix, which influences the actuation rate. To incorporate the viscous contribution, Garcia-Gonzalez [7] proposed a continuum model for hard-magnetic soft materials to implement a finite element framework within a thermodynamically consistent system.

For the design and development of actuators that are based on specifically hard-magnetic soft materials, it is necessary to explore the underlying fundamentals of mechanics and concepts of magnetoactive soft materials based on HMSMs. In this regard, [28] presented an asymmetric Cauchy stress tensor based nonlinear field theory of HMSMs for investigating the magnetically induced response of the actuators. The proposed nonlinear field theory became the foundation for the beams made up of HMSMs [25, 22, 19, 3]. Further, [6] improved the proposed formulation of [28] by accounting for the viscoelastic effects and determine the time-dependent dissipative response of the HMSMs. [7] recently presented a nonlinear continuum framework to model the impact of the viscosity on the magneto-mechanical response of the actuator under statically and dynamically applied loading conditions. [15] presented a dissipative model for HMSMs that explored the impact of ferromagnetic hysteresis and particle volume fraction. [26] presented an efficient computational framework to explore the decomposition of the deformation energy into stretching and lattice volumetric changes. [4] proposed a conceptual model to characterize the complex transformations of hard-magnetic soft beams. Further, they presented a theoretical 3-dimensional framework to analyze the high strains of HMSM beams and described the design guidelines for the optimization of HMS structures [3]. Furthermore, they developed a theoretical model for capturing the magneto-mechanical response of functionally graded HMS beams [5]. [27] presented a theoretical model based on micromechanics to investigate the influence of the hard-magnetic particles interacting with the soft membrane and its response on the actuation performance of HMSMs. [8] presented a unified FEA model for the investigation of hard and soft particle-based magnetoactive membranes considering the visco-elastic effects to simulate a magnetically driven robotic gripper. Additionally, a detailed review of the modeling and characterization of hard-magnetic soft composites can be recapitulated from the article [13].

Most of the existing literature has focused on the quasi-static mode of deformation. However, the dynamic behavior of the HMSAs has been addressed in a few studies. An early work is presented by Xing and Yong [24] in this regard who developed a lumped parameter dynamic model for a planar HMSA driven by constant and periodic magnetic fields. They modeled the constitutive behavior of HMSMs using the neo-Hookean model of hyperelasticity. [16] developed a command shaping scheme for mitigating the residual vibrations in hard-magnetic soft planar actuators to align their position to the desired. Further, he proposed a theoretical dynamic model for modeling a HMSA considering the effect of strain stiffening and further designed an input-shaping scheme for aligning the dynamic response of the actuator to the desired position without any residual vibrations. In this regard, very recently, some efforts have been made by Nandan et al. [18] to model the viscous effects in order to characterize the relaxation and

dissipation effects under deformation of the HMS actuators when subjected to external mechanical and magnetic loading. Further, he investigated the oscillation modes of the HMSM-based viscoelastic actuator and observed its sub-harmonic, harmonic, and super-harmonic resonant frequencies, neglecting the effect of the polymer chain properties. In addition to this, Nandan et al. [17] investigated that the polymer chains have a limiting length. The inherent characteristics of the polymer chains significantly affect the performance of the smart active material-based soft actuators. Furthermore, relatively few studies have addressed the dynamic behavior of the HMSAs [24, 16, 18]. In the aforementioned theoretical studies, the HMS actuator was considered to operate in isothermal conditions, and the constitutive behavior of HMSMs is modeled, neglecting the thermal properties of the HMS material. However, the actual soft polymer properties are significantly affected by the effect of temperature which transforms the desirable properties of such smart polymers. Further, some experiments suggest that the behavior of the soft material is totally different under varying temperature conditions [21]. Based on the non-equilibrium theory of thermodynamics, temperature affects the dynamic properties and physical interpretation of the hard-magnetic soft materials. To the best of author's knowledge, there is a scarcity of research work that models the dynamic response of the HMS actuator undergoing temperature variation. Therefore, the current work focuses on developing a novel formulation using the Euler-Lagrange equation with the objective of capturing the thermal effect on the nonlinear deformation of HMSAs. For efficient and accurate modeling of the dynamic properties, this study shows how the temperature affects the time-dependent response of the HMS actuator undergoing constant and periodic magnetic loading and in the design of smart and remotely controlled devices. Then, the dynamic oscillation, phase diagrams, and Poincare´ maps of the viscoelastic elastomer are studied. A detailed analysis shows the influence of the temperature, frequency, and viscoelasticity on the dynamic stability and the hysteresis.

The current study is structured into the following sections. 2 presents the problem definition and describes the thermoelastic material model utilized to investigate the effect of temperature on the transient response of an HMS actuator. 3 outlines the derivation of the governing equations characterizing the dynamic motion using the principle of least action based on Euler-Lagrange's equation. 4 explores the effect of temperature and prestress on the nonlinear dynamic response of the HMS actuator under a constant and periodic magnetic flux density. Finally, 5 discusses the noticeable inferences drawn from the current work.

2 Problem description

In this study, we consider a typical planar model of the HMSA as depicted in fig. (1a). The coordinates $[X_1, X_2, X_3]$ and $[x_1, x_2, x_3]$ denote the coordinate of a material point in the reference and the spatial configurations, respectively. The initial geometrical dimensions of the actuator in the principal directions prior to deformation are $2L_1 \times 2L_2 \times 2H$. We assume that the actuator undergoes homogeneous deformation when subjected to in-plane equal biaxial mechanical forces (P_1 and P_2) in the X_1 and X_2-directions, respectively, and the magnetic flux density vector ($\mathbf{B}_{\text{applied}}$) in the X_3-direction as shown in 1(b-c). Meanwhile, the operating temperature varies from T_0 to T. The dimensions of the actuator in the spatial configuration are denoted as $2l_1 \times 2l_2 \times 2h$. Following the principles of continuum mechanics, the motion of the planar actuator or the relation between the spatial and the reference co-ordinates is expressed as

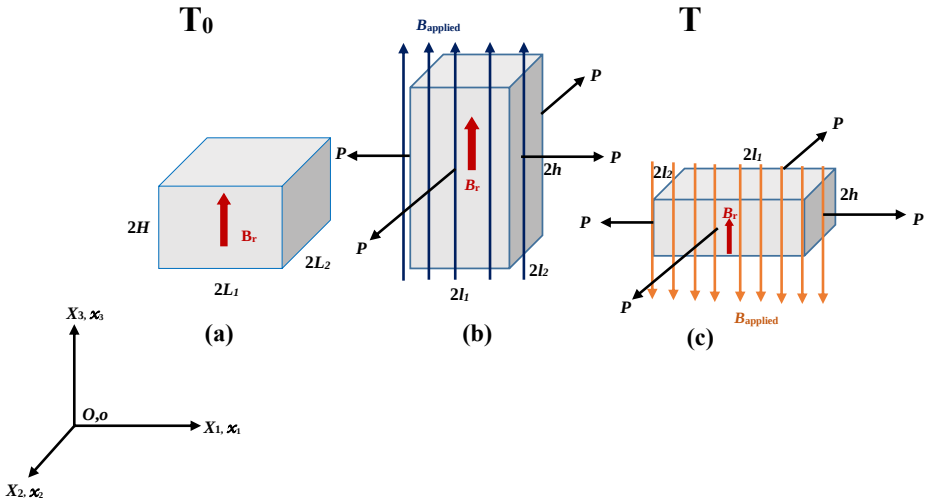

Figure 1: Schematic of the deformation of a planar hard-magnetic soft actuator subjected to an equal bi-axial mechanical loading (P) and a magnetic flux density (B_{applied}).

$$\lambda_i(t) = \frac{x_i(X_1, X_2, X_3, t)}{X_i} \tag{1}$$

where $\lambda_i(t)$ being the function of time only represents the principal stretches along the X_i directions, respectively. Following the incompressibility constraints, the stretch in X_3-direction will be $\lambda_1^{-1}\lambda_2^{-1}$ and in-plane nominal stresses are given by $\sigma_1 = \dfrac{P_1}{L_2 H}$ and $\sigma_2 = \dfrac{P_2}{L_1 H}$ in the X_1 and X_2-directions, respectively.

The applied magnetic field vector $\mathbf{B}_{\text{applied}}$, the residual magnetic flux density vector $\mathbf{B}_{\text{r}}$, and the deformation gradient tensor $\mathbf{F}$, respectively, are defined as

$$\mathbf{B}_{\text{applied}} = \begin{bmatrix} 0 \\ 0 \\ B_{\text{applied}} \end{bmatrix}, \quad \mathbf{B}_{\text{r}} = \begin{bmatrix} 0 \\ 0 \\ B_{\text{r}} \end{bmatrix}, \quad \mathbf{F} = \begin{bmatrix} \lambda_1 & 0 & 0 \\ 0 & \lambda_2 & 0 \\ 0 & 0 & \lambda_1^{-1}\lambda_2^{-1} \end{bmatrix}. \tag{2}$$

We adopted an incompressible neo-Hookean model of hyperelasticity [28] for modeling two nonlinear springs of the Zener rheological model. The damper is characterized by a parameter η. Based on the neo-Hookean model and additive decomposition of total strain energy into isotropic equilibrium and inelastic parts, the total strain energy density (per unit volume) of the material model is written as

$$\Psi_{\text{strain}} = \underbrace{\frac{\mu}{2}\left(\lambda_1^2 + \lambda_2^2 + \lambda_1^{-2}\lambda_2^{-2} - 3\right)}_{\text{Equilibrium}} \tag{3}$$

where μ represents the shear modulus.

The work done by the bi-axial forces P acting perpendicular to the applied magnetic flux density is expressed as

$$WP = 8L_1L_2H\left[\sigma_1\left(\lambda_1 - 1\right) + \sigma_2\left(\lambda_2 - 1\right)\right] \tag{4}$$

where $\sigma_1 = \dfrac{P}{4L_2H}$ *and* $\sigma_2 = \dfrac{P}{4L_1H}$.

In our work, the HMS actuator is subjected to a homogeneous, equi-biaxial force P, so the nonlinear governing equation can be defined using $\sigma_1 = \sigma_2 = \sigma$ and incompressibility constraint $\lambda_1 = \lambda_2 = \lambda$ in 4. Now, the dynamic equation can be given as

$$\Psi_{\text{strain}} = \frac{\mu}{2}\left(2\lambda^2 + \lambda^{-4} - 3\right), \tag{5a}$$

$$W = 8HL^2\left[2\sigma\left(\lambda - 1\right)\right] \tag{5b}$$

The specific free energy density function of a thermoelastic hard-magnetic soft polymer is given as

$$\Psi(\lambda, T) = \frac{T}{T_0}\Psi_{\text{strain}}(\lambda) + \rho c\left[T - T_0 - T\ ln\ \left(\frac{T}{T_0}\right)\right]. \tag{6}$$

We adopted an ideal thermoelastic hard-magnetic soft material model [28], and its free energy density is written as

$$\Psi = \Psi(\lambda, T) - \frac{\mathbf{F}\mathbf{B}_{\text{r}} \cdot \mathbf{B}_{\text{applied}}}{\mu_0} = \Psi(\lambda, T) - \frac{B_{\text{r}}B_{\text{applied}}}{\lambda^2\mu_0}, \tag{7}$$

where μ_0 denotes the vacuum permeability.

In the subsequent section, using the Euler-Lagrange equation of motion along the material model presented in this section, we devise the equations governing the nonlinear dynamics of the HMS actuators.

3 Dynamic governing equations

We devise the ordinary differential equations (ODEs) governing the dynamic characteristics of the considered planar viscoelastic HMSA using the non-conservative form of the Euler-Lagrange equation of motion

$$\frac{d}{dt}\left(\frac{\partial L}{\partial \dot{\lambda}}\right) - \frac{\partial L}{\partial \lambda} + \frac{\partial D}{\partial \dot{\lambda}} = 0; \tag{8}$$

where $\dot{\lambda}$ denotes the time derivatives of the total stretch parameter λ; $(L = T - U)$ signifies the Lagrangian, where T and U are the total kinetic and the potential energies of the actuator, respectively; and D is the energy dissipation function.

Upon integrating the free energy function (6) over the deformed configuration of the actuator, the total strain energy of the actuator is obtained as

$$SE = \int \psi dx_1 dx_2 dx_3 = 8HL^2 \left[\frac{T}{T_0} \frac{\mu}{2} \left(2\lambda^2 + \lambda^{-4} - 3 \right) + \rho c \left[T - T_0 - T \; ln \; \left(\frac{T}{T_0} \right) \right] - \frac{B_{\mathrm{r}} B_{\mathrm{applied}}}{\lambda^2 \mu_0} \right]. \tag{9}$$

Defining the work potential due to external mechanical prestress i.e., $WP = -W$ and using SE expression from 11, the total potential energy of the actuator is expressed as follows

$$U = SE + WP = 8HL^2 \left[\frac{T}{T_0} \left(\frac{\mu}{2} \left(2\lambda^2 + \lambda^{-4} - 3 \right) \right) + \rho c \left[T - T_0 - T \; ln \; \left(\frac{T}{T_0} \right) \right] - 2\sigma \left(\lambda - 1 \right) - \frac{B_{\mathrm{r}} B_{\mathrm{applied}}}{\lambda^2 \mu_0} \right], \tag{10}$$

The expression for the kinetic of the actuator is obtained as follows

$$T = \int \frac{1}{2} \rho \left(\dot{x}_1^2 + \dot{x}_2^2 + \dot{x}_3^2 \right) dx_1 dx_2 dx_3, \tag{11}$$

where ρ denotes the mass density of the HMSM. Inserting the expressions for the spatial coordinates from 2 into 10 and evaluating the integration over the deformed actuator configuration, the kinetic energy of the actuator in terms of stretch rate and stretch parameter is written as [20, 11]

$$T = 8HL^2 \left(\frac{1}{3} \rho \dot{\lambda}^2 L^2 + \frac{2}{3} \rho H^2 \left(\frac{\dot{\lambda}^2}{\lambda^6} \right) \right). \tag{12}$$

Substituting Eqs. 11-12 into 10, the system of ordinary differential equations governing the dynamic behavior of viscoelastic hard-magnetic soft planar actuator is obtained as

$$\ddot{\lambda} \left(\rho L^2 + \frac{2\rho H^2}{\lambda^6} \right) - 6\rho H^2 \left(\frac{\dot{\lambda}^2}{\lambda^7} \right) + 3 \left[\; \mu \left(\frac{T}{T_0} \right) \left(\lambda - \lambda^{-5} \right) - \sigma + \frac{B_{\mathrm{r}} B_{\mathrm{applied}}}{\lambda^3 \mu_0} \; \right] = 0, \tag{13}$$

In this analysis, we consider that the actuator starts from the rest configuration, and the initial conditions corresponding to the rest position are characterized as follows

$$\lambda|_{t=0} = 1; \qquad \left. \frac{\mathrm{d}\lambda}{dt} \right|_{t=0} = 0, \tag{14}$$

In the upcoming section, we will investigate the effect of viscoelasticity on the dynamic behavior of a hard magnetic soft actuator subjected to the constant and the periodic magnetic loading conditions using the governing differential equations (12) and initial conditions (13).

4 Results and analysis

We now perform a parametric study for elucidating how the temperature rise in the HMSM and prestress affect the dynamic response of the planar HMSA. We will utilize the dimensionless quantities for conducting the dynamic analysis. By defining the following dimensionless quantities

$$c = H^2/L^2; \;\; S = \sigma/\mu; \;\; \tau = t\sqrt{\mu/\rho L^2}; \;\; b^2 = \frac{B_{\mathrm{r}} B_{\mathrm{applied}}}{\mu\mu_0}, \tag{15}$$

the governing differential equations (13) and the initial conditions (14) are expressed in the nondimensional form as follows

$$\frac{\mathrm{d}^2\lambda}{\mathrm{d}\tau^2}\left(1+\frac{2c}{\lambda^6}\right) - \left(\frac{\mathrm{d}\lambda}{\mathrm{d}\tau}\right)^2 \frac{6c}{\lambda^7} + 3\left[\left(\frac{T}{T_0}\right)\left(\lambda-\lambda^{-5}\right) - S + b^2\lambda^{-3}\right] = 0, \tag{16}$$

$$\lambda|_{\tau=0} = 1; \qquad \left.\frac{\mathrm{d}\lambda}{d\tau}\right|_{\tau=0} = 0, \tag{17}$$

respectively, where τ is the dimensionless time parameter, c denotes a geometrical constant, S is the dimensionless mechanical pre-stress, and b^2 denotes the dimensionless magnetic flux density. Here, it is worth noting that dimensionless magnetic flux density takes a negative value $b^2 < 0$, when the direction of the applied magnetic flux density is opposite to the direction of residual magnetic flux density and the last term in 16 will be negative. In the present analysis, dimensionless constants c are taken to be 1. We solved the aforementioned governing ODEs (16) along with the initial conditions (17) using fourth-order Runge-Kutta method implemented in MATLAB with ODE 45 solver. Further, we identify the nonlinear oscillations using time history responses, phase-plane portraits, and Poincaré maps. In time history response plots, the stretch in the x_3 direction $\lambda_3 = \lambda^{-2}$ is plotted with the dimensionless time (τ) while phase-portraits plot the stretch rate $\dot{\lambda}_3$ with stretch λ_3. The Poincaré maps are obtained by selecting the period of applied dimensionless magnetic flux density as a time step. The time history response shows periodic motion when it presents predictable and regular trajectories, the Poincaré portrait consists of a single point, and the phase-plane plot represents a closed loop. In contrast, a quasi-periodic motion is defined when the time history response shows an irregular trajectory, the appearance of a torus-shape in phase-plane portrait, and a closed curve of points in the Poincaré map [2, 24, 1, 12, 10].

4.1 Response of actuator under constant magnetic flux density applied along the residual magnetic flux density

In the first case, the HMS actuator was subjected to a constant magnetic flux density in the same direction as the residual magnetic flux density ($b^2 > 0$). We will now analyze the dynamic behavior of the hard-magnetic soft actuator for three different temperatures: 250K, 350K, 400K. 2 shows the time history response of the HMS actuator in the x_3-direction stretch with dimensionless time for different levels of temperature with equi-biaxial prestress (S = 1) and without prestress (S = 0). It is evident from 2 that for any level of temperature in both conditions, the x_3-direction stretch has the same trend and does not reach the equilibrium condition over time. The planar actuator oscillates from the initial configuration to the final equilibrium for different temperature levels in both conditions, indicating a significant effect of the temperature. Further, it can be observed that the magnitude of the cyclic actuation stretch is more at 250K than that of at 350K and 400K. Now, it can be deduced that the deformation decreases with an increase in temperature.

The phase-plane plots were used to evaluate the effect on nonlinear behavior of the HMS actuator by characterizing the stretch rate ($d\lambda_3/d\tau$) to x_3-direction stretch (λ_3). Figure (4)

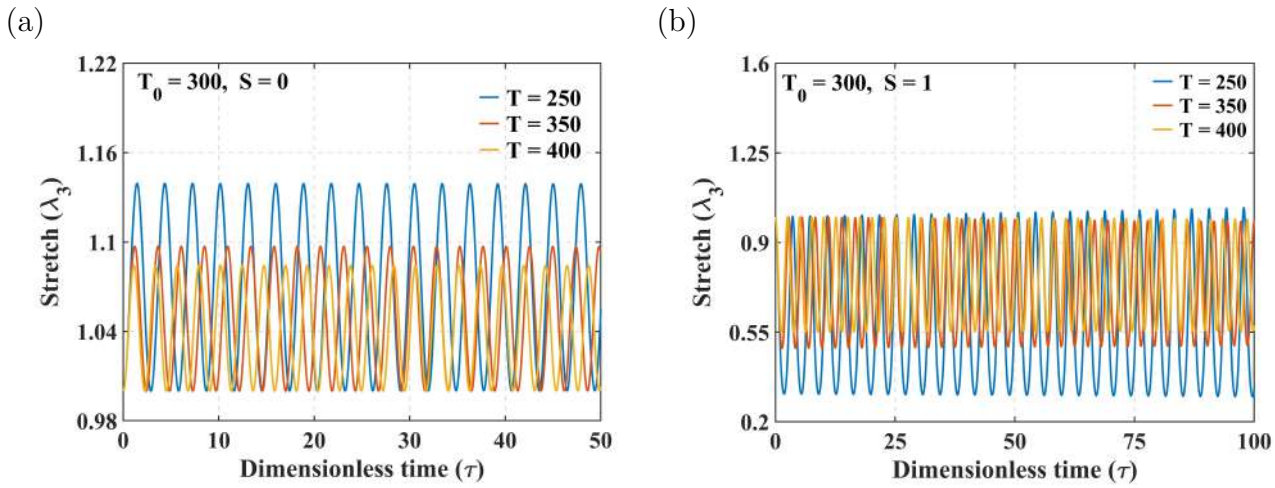

Figure 2: Time-history response of the hard-magnetic soft actuator with respect to different temperature levels (T) under constant magnetic flux density $b = 0.4$ [$b^2 > 0$] and prestress level (a) ($S = 0$), and (b) ($S = 1$).

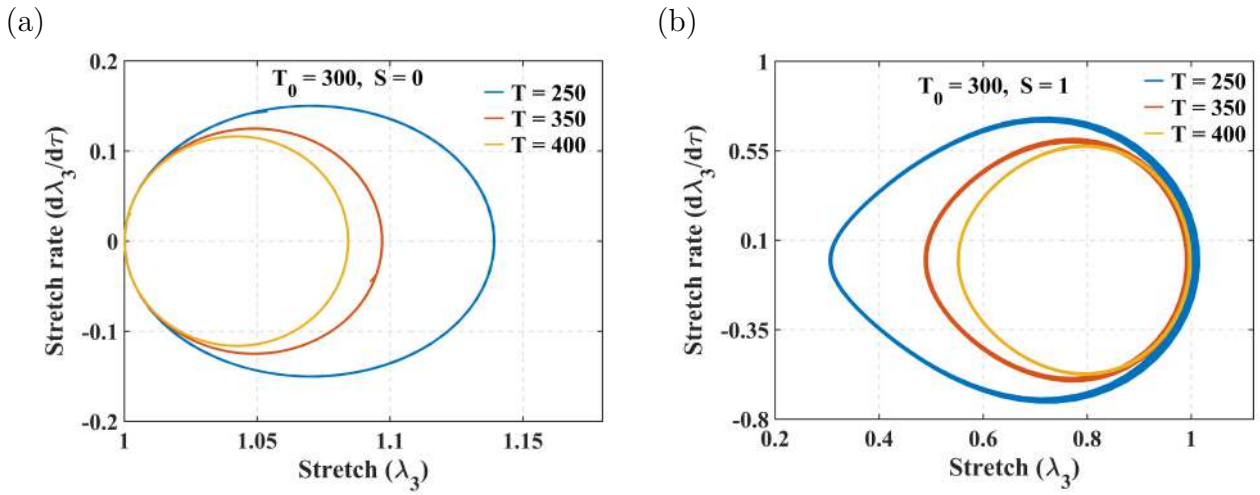

Figure 3: Phase-plane portraits of the hard-magnetic soft actuator with and without bi-axial prestress (S) and under constant magnetic flux density $b = 0.4$ [$b^2 > 0$] and for varying temperature levels (a) $S = 0$ and (b) $S = 1$.

illustrates that the planar actuator oscillates for both prestress and without prestress conditions and forms a closed loop. It is evident that the actuator expands in the x_3 direction ($\lambda_3 > 1$) under magnetic loading without mechanical prestress ($S = 0$), while experiencing compression ($\lambda_3 < 1$) with prestress ($S = 1$) for ($b^2 > 0$). This finding indicates that the effect of prestress (mechanical loading) causes significant compressive deformation instead of the expansion caused by magnetic loading. Furthermore, we observed similar oscillation behavior in both the prestressed and without prestress modes of actuation, except for the variation in stretch rate values. In an incompressible HMS actuator, the stretch in x_3-direction decreases with an increase in temperature. This is because the elastic modulus of the material decreases with increasing temperature. When the temperature of an incompressible HMS actuator increases, the actuator tries to vibrate more rapidly. This increased thermal energy causes the material to become more compliant and less resistant to deformation. As a result, the elastic modulus decreases, and the material becomes easier to stretch. So the stretching in an incompressible HMS actuator decreases with an increase in temperature because the increased thermal energy causes the material to become more compliant and less resistant to deformation.

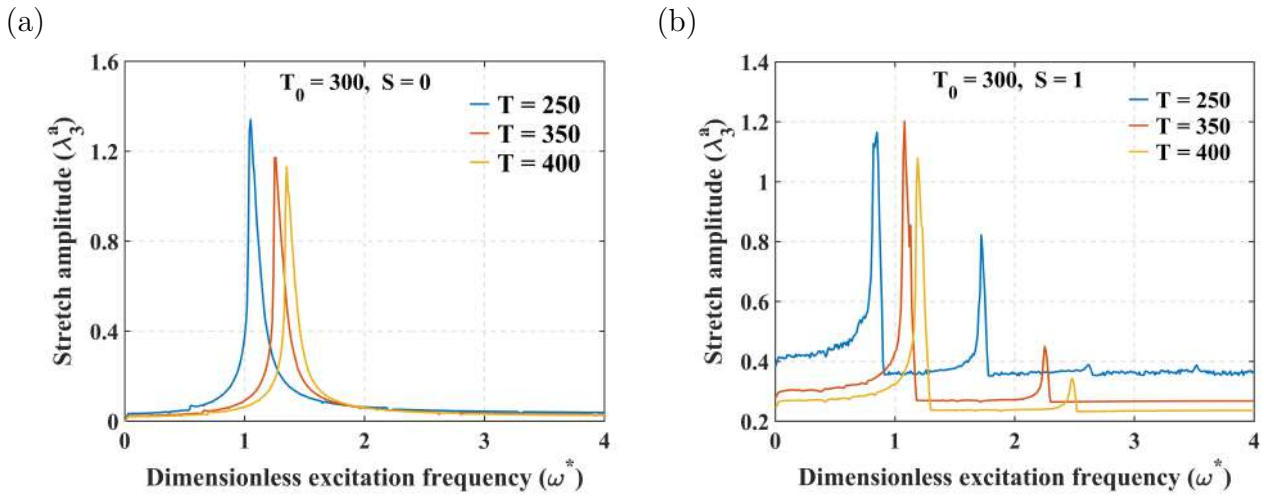

Figure 4: variation of the x_3-direction stretch amplitude with dimensionless excitation frequency ω^* of excitation magnetic flux density for varying temperature and prestress levels (a) ($S = 0$), and (b) ($S = 1$).

In the case of periodic magnetic flux density, the frequency response spectrum is used to characterize the periodic vibration intensity of a hard-magnetic soft (HMS) actuator with three levels of temperature, as shown in 4. It is found that the resonant frequency of the actuator increases with an increase in temperature, while the intensity of vibration decreases. This indicates that temperature enhances the stiffness and modulus of the HMS actuators, resulting in a rise in resonant frequency. However, Increased temperature also yields significant damping that dissipates energy, leading to a decrease in vibration intensity. The resonance properties of the actuator are analyzed, and it is considered that the resonance occurs at the λ_3^a peaks in the frequency range. It is observed that the actuator without prestress (S = 0) shows higher resonant actuation frequency and oscillation amplitude than that of the prestressed actuator (S = 1) for temperature levels of $250K$ and $400K$. However, for $T = 300K$, the actuator without prestress

shows higher resonant actuation frequency and lesser oscillation amplitude than that of the prestressed actuator. The dimensionless resonant frequency for the actuator without prestress with $T = 250K, 350K, 400K$ is calculated to be $\omega_0 = 1.05, 1.25, 1.35$, while the corresponding value for the prestressed case is $\omega_0 = 0.85, 1.08, 1.19$. In 6 (a), it is illustrated that the planar actuator vibrates most strongly and demonstrates the beating phenomenon. For the actuator under periodic magnetic flux density, the beating generally occurs when the frequency of the magnetic flux is close to the natural frequency. Further increases or decrease in temperature, the phenomenon of beating disappears at resonant excitation frequency of 1.25. It can be observed that as the temperature increases, the λ_3^a value decreases gradually without prestress condition while it increases then decreases in prestressed condition, indicating that the effect of strong temperature on nonlinear vibration. As the HMS actuator exhibits strong nonlinear vibrations by increasing the temperature, the nonlinearity of the actuator may be enhanced.

In 6, the time history graph, phase-plane plots, and Poincaré maps for the HMS actuator are presented. The actuator without prestress subjected to an excitation frequency of $\omega^* = 1.25$, which is a resonant excitation frequency at $T = 350K$, is taken into consideration for different temperature levels with the aforementioned actuation conditions. The phase-plane plots and Poincaré maps are plotted to assess the dynamic stability and periodicity of the actuator. The dynamic response of the actuator is demonstrated at a temperature of $T = 250K$ (5(a) and 5(b)), $T = 250K$ (5(c) and 5(d)) and $T = 400K$ (5(e) and 5(f)) without prestress. It can be deduced that all the phase-plane plots do not go to infinity, indicating the stable vibration of HMS actuators. In 5(d), the disordered Poincaré map indicates an aperiodic vibration when $T = 350K$. However, as depicted in 5(b) and 5(f), an increase or decrease in temperature leads to ordered Poincaré maps forming closed loops, which indicate quasi-periodic vibrations. Therefore, the variation of temperature, either an increase or decrease in temperature, tunes the periodicity of the nonlinear vibrations of HMS actuators, resulting in a transition from aperiodic vibration to quasi-periodic vibration.

Further, the actuator is excited with an excitation frequency of $\omega^* = 1.08$, which is also the resonant excitation frequency at $T = 350K$ with prestress conditions. The 6(a) and 6(e) shows that the actuator displays stable periodic oscillations for the temperatures of 250K and 400K, respectively, similar to the obtained actuation mode in the absence of mechanical prestress. Further, it is also examined that the actuator without prestress achieves stability faster than the prestressed actuator.

Furthermore, 6 also illustrates that the actuator exhibits aperiodic oscillation for the temperature of $T = 350K$ at resonant frequency and a stable periodic oscillation for both states of prestress for the crosslinks parameter of $T = 250K$ *and* $400K$ and deviates from its normal response by forming a closed spiral, indicating the occurrence of resonance in the planar actuator. Similar to the earlier cases of $T = 250K, 350K, 400K$, the actuator attenuates the stable periodic oscillations more rapidly in the absence of prestress than the prestressed actuator at resonant excitation frequencies.

It can be inferred from 5(a) and 5(b) that the response of the HMS actuator in the absence of mechanical prestress ($S = 0$) is significantly similar to the prestressed actuator ($S = 1$). The dimensionless excitation frequency of the prestressed HMS actuator rises compared to the actuator without mechanical prestress for the same temperature. The time history graph along with the corresponding phase-plane plots and Poincaré maps also presents similar results for the actuator with mechanical prestress $S = 1$ in comparison to the actuator without mechanical

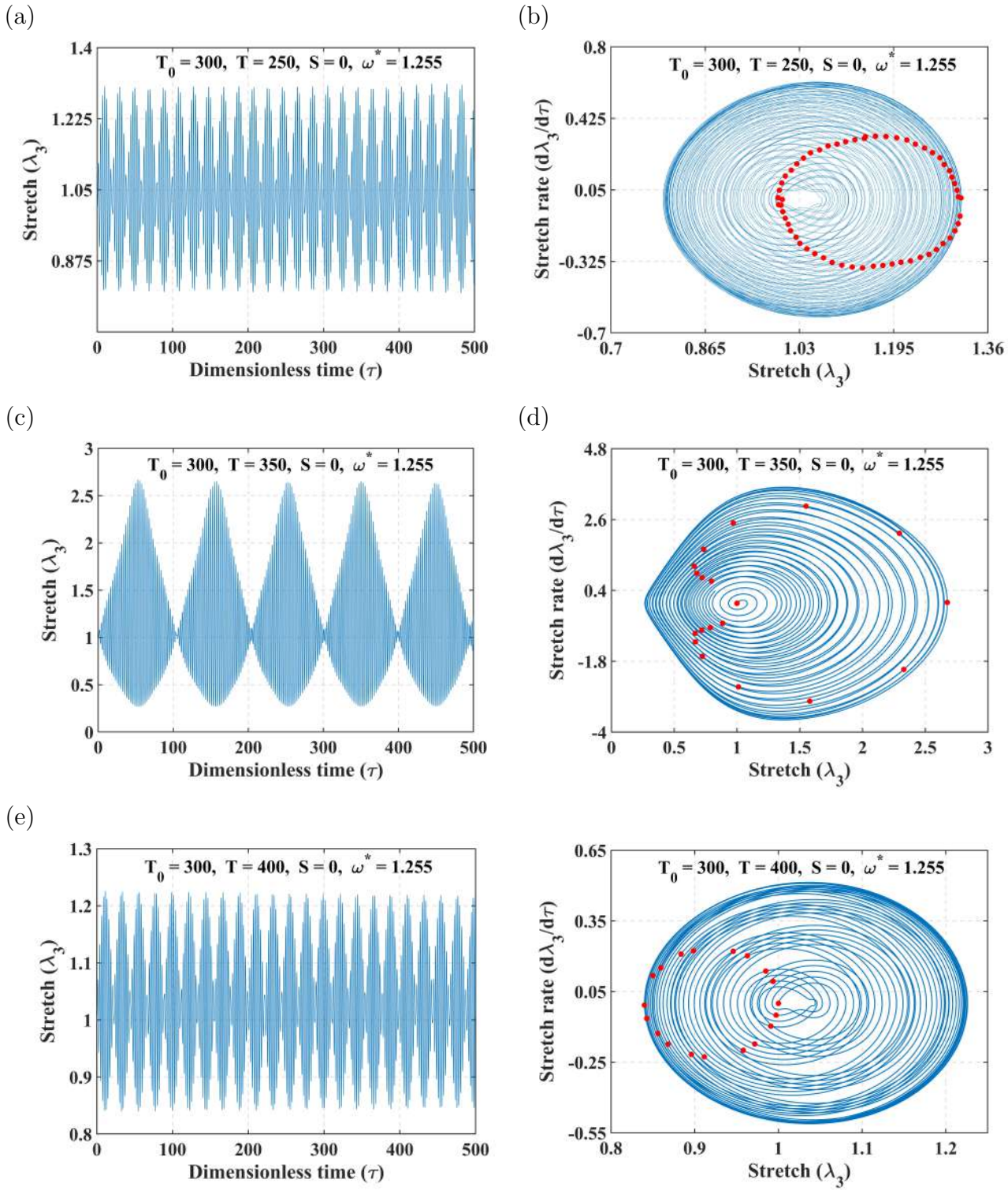

Figure 5: Phase–plane portraits along with Poincaré maps of the actuator without prestress for different levels of temperature levels and and frequency of excitation ω^*.

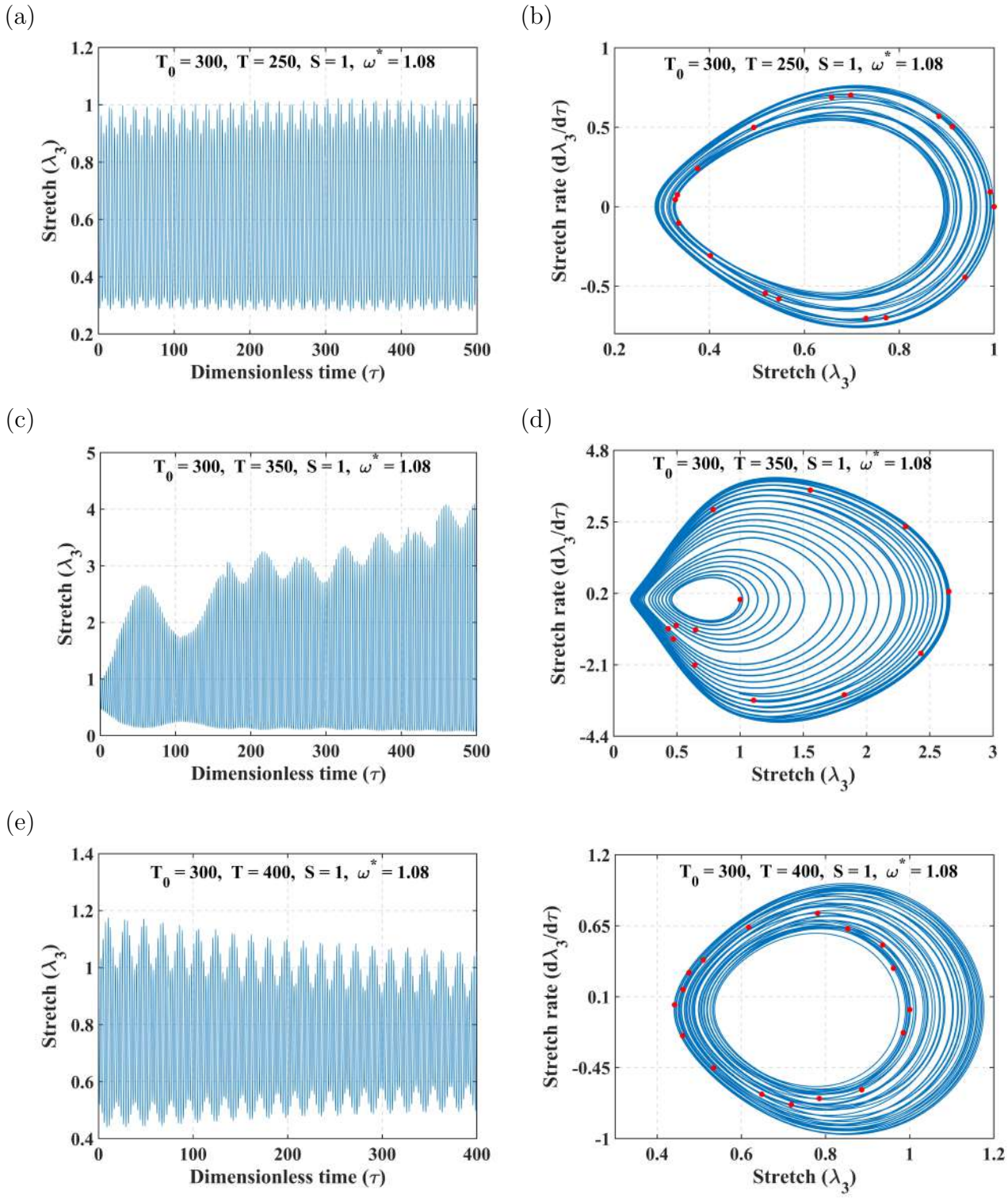

Figure 6: Phase–plane portraits along with Poincaré maps of the actuator with prestress for different levels of temperature levels and and frequency of excitation ω^*.

prestress. This signifies the similar plots shown in 5 and 6.

5 Concluding remarks

In this article, an incompressible hyperelastic thermal based material model was considered to define the constitutive behavior of the HMS actuator. An analytical framework of the HMS actuator is presented by using Lagrange's equation, which considers the effect of temperature to investigate the dynamic stability, periodicity, dynamic response, and resonance properties. The analysis was carried out by varying the level of the material properties for both prestress and without prestress conditions in the dynamic mode of actuation when excited by constant and periodic magnetic fields. The inferences of the study can be summarized as follows:

1. The actuator with prestress condition attains a higher level of deformation at the equilibrium state compared to the case in which actuator is not prestressed for any value of thermal parameter.

2. The actuator with prestress (S= 1) undergoes compression: large compressive deformation because of mechanical loading over expansion due to magnetic loading.

3. This increased thermal energy causes the material to become more compliant and less resistant to deformation. As a result, the elastic modulus decreases, and the material becomes easier to stretch. So the stretching in an incompressible HMS actuator decreases with an increase in temperature because the increased thermal energy causes the material to become more compliant and less resistant to deformation.

4. In this analysis, the actuator undergoes oscillations from initial configuration to final configuration and increase in temperature reduces oscillation stretch.

5. The variation of temperature, either an increase or decrease in temperature, tunes the periodicity of the nonlinear vibrations of HMS actuators, resulting in a transition from aperiodic vibration to quasi-periodic vibration.

The underlying analytical model, along with the inferences reported in the current analysis, can help to understand the dynamic behavior of the thermal effects and serve as a guide in the design and development of the futuristic remotely driven soft actuators executing time-dependent motion.

Acknowledgment

The authors are thankful to the anonymous reviewer for the valuable inputs. Authors acknowledge the financial support from Department of Science and Technology (DST), India through Grant No. DST/INSPIRE/04/2019/000500, and Science and Engineering Research Board (SERB), India through Start-up Research Grant (SRG/2021/000776).

References

[1] A. Alibakhshi, S. Dastjerdi, B. Akgöz, and Ö. Civalek. Parametric vibration of a dielectric elastomer microbeam resonator based on a hyperelastic cosserat continuum model. *Composite Structures*, 287:115386, 2022.

[2] H. W. Broer, G. B. Huitema, and M. B. Sevryuk. *Quasi-periodic motions in families of dynamical systems: order amidst chaos*. Springer, 2009.

[3] W. Chen, L. Wang, Z. Yan, and B. Luo. Three-dimensional large-deformation model of hard-magnetic soft beams. *Composite Structures*, 266:113822, 2021.

[4] W. Chen, Z. Yan, and L. Wang. Complex transformations of hard-magnetic soft beams by designing residual magnetic flux density. *Soft Matter*, 16(27):6379–6388, 2020.

[5] W. Chen, Z. Yan, and L. Wang. On mechanics of functionally graded hard-magnetic soft beams. *International Journal of Engineering Science*, 157:103391, 2020.

[6] F. Dadgar-Rad and M. Hossain. Large viscoelastic deformation of hard-magnetic soft beams. *Extreme Mechanics Letters*, page 101773, 2022.

[7] D. Garcia-Gonzalez. Magneto-visco-hyperelasticity for hard-magnetic soft materials: theory and numerical applications. *Smart Materials and Structures*, 28(8):085020, 2019.

[8] C. Kadapa and M. Hossain. A unified numerical approach for soft to hard magneto-viscoelastically coupled polymers. *Mechanics of Materials*, 166:104207, 2022.

[9] K. A. Kalina, J. Brummund, P. Metsch, M. Kästner, D. Y. Borin, J. Linke, and S. Odenbach. Modeling of magnetic hystereses in soft mres filled with ndfeb particles. *Smart Materials and Structures*, 26(10):105019, 2017.

[10] A. Khurana, A. Kumar, S. K. Raut, A. K. Sharma, and M. M. Joglekar. Effect of viscoelasticity on the nonlinear dynamic behavior of dielectric elastomer minimum energy structures. *International Journal of Solids and Structures*, 208:141–153, 2021.

[11] A. Khurana, A. Kumar, A. K. Sharma, and M. M. Joglekar. Effect of polymer chains entanglements, crosslinks and finite extensibility on the nonlinear dynamic oscillations of dielectric viscoelastomer actuators. *Nonlinear Dynamics*, 104(2):1227–1251, 2021.

[12] A. Kumar, A. Khurana, A. K. Sharma, and M. Joglekar. An equivalent spring-based model to couple the motion of visco-hyperelastic dielectric elastomer with the confined compressible fluid/air mass. *International Journal of Non-Linear Mechanics*, 147:104232, 2022.

[13] S. Lucarini, M. Hossain, and D. Garcia-Gonzalez. Recent advances in hard-magnetic soft composites: Synthesis, characterisation, computational modelling, and applications. *Composite Structures*, 279:114800, 2022.

[14] G. Z. Lum, Z. Ye, X. Dong, H. Marvi, O. Erin, W. Hu, and M. Sitti. Shape-programmable magnetic soft matter. *Proceedings of the National Academy of Sciences*, 113(41):E6007–E6015, 2016.

[15] D. Mukherjee, M. Rambausek, and K. Danas. An explicit dissipative model for isotropic hard magnetorheological elastomers. *Journal of the Mechanics and Physics of Solids*, 151:104361, 2021.

[16] N. Nagal, S. Srivastava, C. Pandey, A. Gupta, and A. K. Sharma. Alleviation of residual vibrations in hard-magnetic soft actuators using a command-shaping scheme. *Polymers*, 14(15):3037, 2022.

[17] S. Nandan, D. Sharma, and A. K. Sharma. Dynamic modeling of hard-magnetic soft actuators: Unraveling the role of polymer chain entanglements, crosslinks, and finite extensibility. *Journal of Magnetism and Magnetic Materials*, 587:171237, 2023.

[18] S. Nandan, D. Sharma, and A. K. Sharma. Viscoelastic effects on the nonlinear oscillations of hard-magnetic soft actuators. *Journal of Applied Mechanics*, 90(6):061001, 2023.

[19] A. Rajan and A. Arockiarajan. Bending of hard-magnetic soft beams: A finite elasticity approach with anticlastic bending. *European Journal of Mechanics-A/Solids*, 90:104374, 2021.

[20] A. K. Sharma, S. Bajpayee, D. M. Joglekar, and M. M. Joglekar. Dynamic instability of dielectric elastomer actuators subjected to unequal biaxial prestress. *Smart Materials and Structures*, 26(11):115019, 2017.

[21] J. Sheng, H. Chen, B. Li, and L. Chang. Temperature dependence of the dielectric constant of acrylic dielectric elastomer. *Applied Physics A*, 110:511–515, 2013.

[22] L. Wang, Y. Kim, C. F. Guo, and X. Zhao. Hard-magnetic elastica. *Journal of the Mechanics and Physics of Solids*, 142:104045, 2020.

[23] S. Wu, Q. Ze, R. Zhang, N. Hu, Y. Cheng, F. Yang, and R. Zhao. Symmetry-breaking actuation mechanism for soft robotics and active metamaterials. *ACS applied materials & interfaces*, 11(44):41649–41658, 2019.

[24] Z. Xing and H. Yong. Dynamic analysis and active control of hard-magnetic soft materials. *International Journal of Smart and Nano Materials*, 12(4):429–449, 2021.

[25] D. Yan, A. Abbasi, and P. M. Reis. A comprehensive framework for hard-magnetic beams: reduced-order theory, 3d simulations, and experiments. *International Journal of Solids and Structures*, 257:111319, 2022.

[26] H. Ye, Y. Li, and T. Zhang. Magttice: a lattice model for hard-magnetic soft materials. *Soft Matter*, 17(13):3560–3568, 2021.

[27] R. Zhang, S. Wu, Q. Ze, and R. Zhao. Micromechanics study on actuation efficiency of hard-magnetic soft active materials. *Journal of Applied Mechanics*, 87(9), 2020.

[28] R. Zhao, Y. Kim, S. A. Chester, P. Sharma, and X. Zhao. Mechanics of hard-magnetic soft materials. *Journal of the Mechanics and Physics of Solids*, 124:244–263, 2019.